APPLIED MECHANICS

Запропоновано підходи щодо аналітичних оцінок моменту інерції зігнутих ділянок бурильної колони при її обертанні. Дослідження обертання криволінійних ділянок бурильної колони на даний час пов'язані з певними труднощами, які виникають через відсутність точних виразів для оцінки моментів інерції зігнутої труби за параметрами її деформації. Вирішення таких завдань є важливими для аналізу динамічної стійкості бурильних колон при роторному і роторно-турбінному способах буріння при дослідженнях напружено-деформованого стану її елементів, уточнення енергетичних затрат на процес обертання зігнутих ділянок у свердловині, а також аналізу критичних частот обертання. Проведено дослідження моменту інерції зігнутої ділянки бурильної колони на моделях із зосередженими та розподіленими масами. На основі цього встановлено точні та асимптотичні аналітичні залежності для визначення інерційних характеристик криволінійних ділянок бурильної колони та подано рекомендації щодо застосування цих залежностей.

Сучасною тенденцією розвитку і модернізації бурового обладнання є застосування бурильних труб, виготовлених із нетрадиційних матеріалів. Враховуючи науковий і практичний інтерес до застосування цих матеріалів, проведено розрахунки моментів інерції для зігнутих ділянок бурильних колон, що можуть комплектуватися сталевими, алюмінієвими, титановими чи склопластиковими бурильними трубами. Аналітичне оцінювання моменту інерції зігнутих ділянок відноситься до різного масштабу деформованого стану бурильної колони. Формула моменту інерції, встановлена на простих моделях, є коректною у тих випадках, коли криволінійна ділянка бурильної колони зазнає великих переміщень. У випадку малих переміщень слід застосовувати аналітичний результат, здобутий на моделі із розподіленими параметрами. Встановлені закономірності є важливими для аналізу динаміки бурильної колони в глибоких умовно вертикальних, похило-скерованих чи горизонтальних свердловинах із складним гірничо-геологічним профілем

Ключові слова: бурильна колона, бурильна труба, зігнутий стержень, зосереджена маса, розподілена маса, момент інерції

UDC 622.24.058
DOI: 10.15587/1729-4061.2019.154827

ANALYTICAL ESTIMATION OF INERTIAL PROPERTIES OF THE CURVED ROTATING SECTION IN A DRILL STRING

Ja. Grydzhuk
PhD, Associate Professor
Department of Technical Mechanics*
E-mail: jaroslav.gridzhuk@gmail.com
I. Chudyk
Doctor of Technical Sciences, Professor
Department of Well Drilling*
E-mail: chudoman@ukr.net
A. Velychkovych
PhD, Associate Professor
Department of Building Mechanics*
E-mail: a_velychkovych@ukr.net
A. Andrusyak
PhD, Associate Professor
Department of Building Mechanics*
E-mail: pirelliandgoodri@ukr.net
*Ivano-Frankivsk National Tachnical Univercity of Oil and Gas
Karpatska str., 15, Ivano-Frankivsk, Ukraine, 76019

1. Introduction

The commonly adopted world-wide practice that continues to develop at present is the directed drilling of deep oil and gas wells at which the axis of a bore often happens to be a spatial curve. In this case, a string of drill pipes is a rather complex spatial system with distributed parameters. Depending on the magnitude of external and volumetric loads, as well as the conditions of contact interaction with the wall of the well, a string or its individual sections may experience phenomena that are characteristic of classic elastic rods. Specifically, a string can acquire a spiral-like shape, undergo local loss of stability, execute longitudinal, twisting or transverse oscillations. In addition, in the void of a curvilinear borehole a drill string is exposed to the action of friction and contact forces, the forces of inertia from a washing fluid, etc. The listed phenomena exert a negative impact on the elements of a drill string, bits, downhole motors, and in general lead to a loss of energy and reduce the techno-economic indicators of drilling [1–4].

To refine the parameters of loading and the stressed-deformed state of a drill string, it is necessary to have a well-defined procedure for determining the moments of inertia of its curved sections. Therefore, it is a relevant task for the theory of dynamic stability of elastic systems to investigate the inertial properties of a curvilinear string of pipes at rotation. The solution to this problem is necessary in order to properly conduct a dynamic analysis of drill strings at rotor and rotor-turbine drilling techniques.

2. Literature review and problem statement

Estimation approaches to the theory of rods have been developed quite well, however, when studying the processes of rotation of the curved sections of a drill string, there are certain difficulties related to the lack of precise expressions to evaluate the moment of inertia of a bent pipe based on the parameters of its deformation. Resolving such problems is required to evaluate the dynamic stability and pliability of a drill string under conditions of the non-stationary vibration load when drilling deep wells and, particularly, wells with difficult mining and geological conditions [4–6].

Most researchers tried to avoid taking into consideration the influence of the curvilinearity at sections in a drill string on its inertial properties at rotation, neglecting this influence completely, or using a series of assumptions [2, 4]. That created the problem for a dynamic analysis of long strings at rotation because of a mismatch between real objects and mathematical models [7]. Excessive schematization of the behavior of these mechanical systems simplifies the solutions to problems, but reduces the accuracy of results, and vice versa. In this case, each proposed engineering model, which is based on a series of hypotheses and assumptions, requires verification through numerical methods [8] or experiment [9].

The features of approaches to the dynamic analysis of a drill string depend on the shape of its elastic equilibrium, which, as a result of the diversity of technical- technological and mining-geological factors, can be both flat and spatial [10]. Paper [11] described an analogy between the phenomena of loss of stability when long rods are compressed and when flexible shafts reach the critical frequency of rotation; it also outlined approaches to practices aimed at preventing these dangerous states. Based on the research results, the authors proposed techniques for creating critical-free rotors, resonance-free structures and rods that do not lose stability when compressed.

Some authors [5, 12] believe that reducing the vibrations of drilling equipment might be the key to maintaining the dynamic stability of a drill string in general. The relevant issues on designing vibration protection devices for long structures (drill strings, pump-and-compressor rods) were considered in papers [13–15]. Specifically, study [13] presented designs of inertial devices to control the dynamic mode of a drill string, which simultaneously act as collared drill pipes. They are executed in the form of a single-section or multi-section hollow body partially filled with a loose medium. Paper [14] addresses the development of shell elastic elements for the strings of pump-and-compressor rods. A special feature of the proposed designs is the optimal combination of amortization and damping properties, which makes it possible to significantly reduce the dynamic loads on a string of rods. Authors of work [15] employed the effects that are based on the phenomenon of antiresonance to develop a broadband vibration damper for the long elements of structures.

Modeling of contact interaction in the shell-rod systems (the type of rod-rigid ferrule, elastic body-cylindrical shell) at monotonous loading in order to determine the strength, rigidity and damping capacity of these systems was performed in papers [16–19]. Drilling shock absorbers with solid shells were considered in [16], hydro-elevators and ring compensators – in papers [17, 18], authors of [19] examined the dampers that were designed based on the cut shells.

The phenomenon of contact interaction between the elements of a drill string and the wall of a well is a key factor that determines the energy intensity of drilling process at string rotation. For this area, it remains relevant to mathematically model the static and dynamics of rod systems regarding the tasks on eliminating the pinching of a drill string [20–22]. Refinement of models of interaction between the surface of a rod and the elastic or non-elastic environment is required for the safe operation of long objects. The use of such models is relevant for pipelines in the areas of soil displacement [23], in places where a damaged base is mobile [24], and where active fault is crossed [25, 26]. Similar models of contacting bodies are applicable to improve the durability of drill strings [27, 28] and to provide quality centering of casing pipes [29].

Specifically, paper [30] analyzed the dynamic behavior of pipelines as a rod system, using the method of dynamic rigidities. It is shown that for curved rods it is advisable to apply a model that consists of straight sections and inertia-free turning elements.

Analytical and experimental research into the dynamics of a flexible shaft rotation in moving supports is reported in [31]. The shaft is modeled in the form of a flexible rod, whose mass is represented in the form of a cylinder located in the place of the largest deflection of the rod. The moment of inertia of such a system is determined similar to a cylinder whose rotation axis is parallel to its central axis. Similar study is reported in [32].

At present, there are known models in which a drill string is represented as a standard rotational pendulum while the layout of the bottom of a string is regarded as a fly-wheel [4]. There are other models with concentrated masses that take into consideration the relationship between oscillations of different classes [2, 4]. There are well-developed models that take into consideration both the vibration of a drill string and the so-called delay effects [2]. The nonlinear models of a drill string [3] are applied in selected areas, as well as models that more or less accurately take into consideration the interaction between a string and the walls of a well [4, 33, 34].

Despite the diversity of mechanical and mathematical solutions, all known models fail to account for changes in the inertial characteristics of a drill string that occur due to bending of pipes. Therefore, taking into consideration the specified characteristics is possible by establishing and investigating analytical dependences for determining the moments of inertia for the curved sections of a drill string at its rotation.

3. The aim and objectives of the study

The aim of this work is to derive and verify analytical dependences to determine the moments of inertia of the curved sections in a drill string at its rotation.

To accomplish the aim, the following tasks have been set:

– to explore the inertial properties of the curved section in a drill string at rotation by using models with concentrated masses;

– to explore the inertial properties of the curved section in a drill string at rotation by using a model with distributed masses;

– to justify recommendations for the application of exact and asymptotic results of research;

– to carry out numerical calculations and to perform a comparative analysis of the moments of inertia of curvilin-

ear strings, equipped with drill pipes made from different materials.

4. Studying the inertial properties of the curved section in a drill string at its rotation by using models with concentrated masses

Let the mass of a tubular rod be evenly distributed along the curve S (Fig. 1, *a*), whose axis shape is described by an arbitrary function $y(x)$. For example, it could be a sinusoidal or a cosine function if drill pipes are in the compressed part of the string, a hyperbolic function if they are in the stretched one, etc. Curve S rotates around the x axis at an arbitrary angular speed. For certainty, we shall accept that outline of the axis of curve S is described by a sinusoidal function:

$$y(x)=f\sin\frac{\pi x}{L}, \tag{1}$$

where L is the length of the deflection halfwave; f is the magnitude of the maximum deflection.

In further calculations, we represent this material curve in the form of a weightless curve with a focused mass (Fig. 1, *b*). The essence of the proposed model is as follows. The magnitude of concentrated mass $\tilde{M}$ must be chosen so that the inertial properties of the model with a concentrated mass at rotation relative to the x axis are equivalent to the model with distributed parameters.

First, determine the mass of arc S (Fig. 1, *a*):

$$M=\int_0^S m(s)\mathrm{d}s=\int_0^L m(x)\sqrt{1+\left[y'(x)\right]^2}\,\mathrm{d}x=$$
$$=m\int_0^L\sqrt{1+\left(f\frac{\pi}{L}\right)^2\cos^2\left(\frac{\pi}{L}x\right)}\,\mathrm{d}x, \tag{2}$$

where $m(s)$ is the mass per unit of the rod's length;

$$ds=\sqrt{1+\left[y'(x)\right]^2}dx$$

is the differential of the arc of curve $y(x)$;

$$y'(x)=\frac{dy(x)}{dx}=f\frac{\pi}{L}\cos\left(\frac{\pi}{L}x\right).$$

The moment of inertia of arc S relative to the x axis:

$$J_x=\int_0^L y^2(x)m(x)\sqrt{1+\left[y'(x)\right]^2}\,\mathrm{d}x=$$
$$=mf^2\int_0^L\sin^2\left(\frac{\pi x}{L}\right)\sqrt{1+\left(f\frac{\pi}{L}\right)^2\cos^2\left(\frac{\pi}{L}x\right)}\,\mathrm{d}x. \tag{3}$$

Next, we consider a weightless curve S of equivalent concentrated mass $\tilde{M}$ (Fig. 1, *b*). The equivalent moment of inertia for the system of concentrated mass is represented as follows:

$$\tilde{J}_x=\tilde{M}f^2=\zeta Mf^2, \tag{4}$$

where $\tilde{M}$ is the equivalent concentrated mass; ζ is the coefficient of mass reduction.

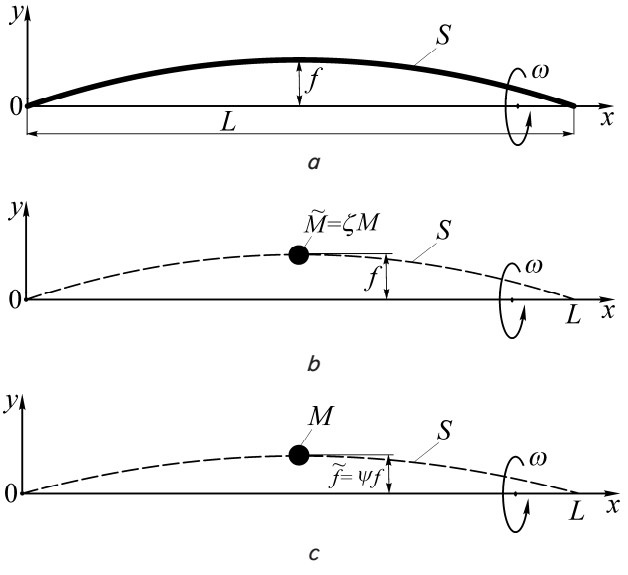

Fig. 1. Models of the bent solid rod: *a* — material curve; *b* — weightless curve of equivalent concentrated mass; *c* — weightless curve of concentrated mass and an equivalent expansion of lift

By assigning to the moment of inertia of arc S the equivalent moment of inertia of the system with the same concentrated mass $\tilde{M}$ from (4), we obtain:

$$\zeta=\frac{J_x}{Mf^2},$$

considering the right-hand parts of expressions (2) and (3), we obtain:

$$\zeta=\frac{\int_0^L\sin^2\left(\frac{\pi x}{L}\right)\sqrt{1+\left(f\frac{\pi}{L}\right)^2\cos^2\left(\frac{\pi}{L}x\right)}\,\mathrm{d}x}{\int_0^L\sqrt{1+\left(f\frac{\pi}{L}\right)^2\cos^2\left(\frac{\pi}{L}x\right)}\,\mathrm{d}x}. \tag{5}$$

Coefficient of mass reduction depends on the geometrical parameters and the deformed state of the rod. Thus, to replace the system (Fig. 1, *a*) with its single-mass equivalent (Fig. 1, *b*), it is necessary to perform the following. First, calculate the mass of material curve M from formula (1). Next, determine the coefficient of mass reduction using expression (5). And, finally, find the equivalent concentrated mass $\tilde{M}=\zeta M$.

For the case $L\gg f$, the result from solving the set problem can be obtained analytically with a high degree of accuracy. Thus, expressions (2) and (3) after integration will take the following form

$$M=mL\left(1+\frac{1}{4}\left[\frac{f\pi}{L}\right]^2+C\left[\frac{f\pi}{L}\right]^4\right), \tag{6}$$

$$J_x=\frac{mf^2L}{2}\left(1+\frac{1}{8}\left[\frac{f\pi}{L}\right]^2+C\left[\frac{f\pi}{L}\right]^4\right), \tag{7}$$

where C is an unidentified magnitude, which is disregarded because at $L\gg f$, the multiplier is very small.

The coefficient of mass reduction in this case will take the following form:

$$\zeta = \frac{1+\frac{1}{8}\left(\frac{\pi f}{L}\right)^2}{2+\frac{1}{2}\left(\frac{\pi f}{L}\right)^2} = \frac{1}{2}\left(1-\frac{1}{8}\left(\frac{\pi f}{L}\right)^2\right). \quad (8)$$

At the second stage, while trying to solve the set problem for cases when $L \gg f$, we apply a slightly different approach. We accept, as a variable parameter, not the mass of a bent rod, but the extension of arc lift of its curved axis *f*. The equivalent system is shown in Fig. 1, *c*. In this case, the equivalent moment of inertia for a single-mass model will be written in the following form:

$$\tilde{J}_x = M\tilde{f}^2 = M(\psi f)^2, \quad (9)$$

where ψ is the coefficient of deflection extension reduction.

$$M(\psi f)^2 = J_x \Rightarrow \psi = \frac{1}{f}\sqrt{\frac{J_x}{M}}. \quad (10)$$

Considering (2) and (3), the coefficient of deflection extension reduction

$$\psi = \sqrt{\frac{\int_0^L \sin^2\left(\frac{\pi x}{L}\right)\sqrt{1+\left(f\frac{\pi}{L}\right)^2\cos^2\left(\frac{\pi}{L}x\right)}\,dx}{\int_0^L \sqrt{1+\left(f\frac{\pi}{L}\right)^2\cos^2\left(\frac{\pi}{L}x\right)}\,dx}}. \quad (11)$$

Dependences (9) to (11) should be used for exact calculations of the moments of inertia of the curved sections in a string. Further numerical check of dependences (5) and (8) shows a high convergence of results. Thus, for the approximate calculations at $f/L < 1/20$ one can affirmatively use formulae (6) to (8).

5. Studying the inertial properties of the curved section in a drill string at its rotation using a model with distributed masses

At this stage of our study, we shall refine the statement of the problem. To this end, assign real transverse dimensions to the material curve. Consider a bent filled tubular rod of length *s*, which rotates around the *x* axis. Density of the material of the rod and the filler are, respectively, ρ_1 and ρ_2, radius of the cross section of the rod is *r*, and the wall thickness is *h*. The elastic line of the rod is described by an arbitrary analytical function *y*(*x*), which we consider to be known. Let this function be represented by expression (1). It is required to calculate the moment of inertia J_x of such an object when it rotates around the *x* axis.

We shall consider that the rod is made up of inhomogeneous rigid thin disks that could be exposed at rod deformation to angular and linear displacements (Fig. 2). The discs in this case remain perpendicular to the axis of the rod, and because we look at small deflections, the distortions of cross sections and the ovalization are disregarded.

The moment of inertia of an arbitrary disk relative to the x_1 axis (Fig. 2) will be represented in the form:

$$J_{x\xi} = J_{x1}\cos^2\alpha = \frac{J_{x1}}{1+y'^2}, \quad (12)$$

where

$$\cos^2\alpha = \frac{1}{1+tg^2\alpha} = \frac{1}{1+y'^2}.$$

Then the moment of inertia of an arbitrary disk relative to the *x* axis is:

$$J_x = \frac{J_{x1}}{1+y'^2} + my^2. \quad (13)$$

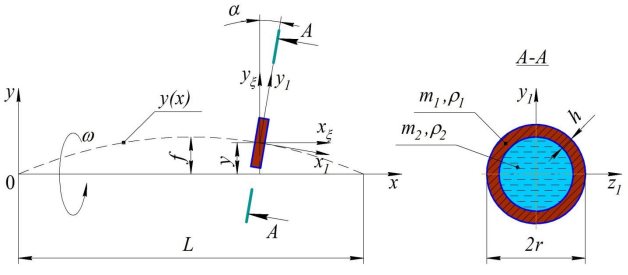

Fig. 2. Model of the filled tubular rod

The moment of inertia of a bent rod:

$$J_x = \int_s \left(\frac{J_{x1}}{1+y'^2} + my^2\right) ds \quad (14)$$

or

$$J_x = \int_L \left(\frac{J_{x1}}{1+y'^2} + my^2\right)\sqrt{1+y'^2}\,dx, \quad (15)$$

where

$$J_{x1} = \frac{1}{2}m_2(r-h)^2 + m_1r^2; \quad m_1 = 2\pi rh\rho_1;$$

$$m_2 = \pi(r-h)^2\rho_2; \quad m = m_1 + m_2.$$

For more specific numerical results, we show the resulting formula:

$$J_x = \int_L \left(\frac{\frac{1}{2}m_2(r-h)^2 + m_1r^2}{1+\left(f\frac{\pi}{L}\right)^2\cos^2\left(\frac{\pi}{L}x\right)} + m\left(f_1' \quad \frac{\pi x}{L}\right)^2\right)\times$$

$$\times\sqrt{1+\left(f\frac{\pi}{L}\right)^2\cos^2\left(\frac{\pi}{L}x\right)}\,dx. \quad (16)$$

Formula (16) is accurate, albeit cumbersome. For practical calculations based on (15), we shall derive a simplified formula. For the case of small deflections and the rod's angles of rotation, we assume that the following inequalities hold:

$$\max_x \frac{y(x)}{r} \ll 1,$$

$$y'(x) \le 1, \quad x \in [0, L].$$

Then

$$\frac{1}{1+y'^2}\approx 1-y'^2,\ \ \sqrt{1+y'^2}\approx 1+\frac{1}{2}y'^2.$$

By retaining in the asymptotic decompositions of expression (15) the magnitudes of the order y'^2 and y^2 only, we obtain:

$$J_x=\int_L\left(\frac{J_{xI}}{1+y'^2}+my^2\right)\sqrt{1+y'^2}\,dx\approx$$
$$\approx\int_L\left(J_{xI}\left(1-y'^2\right)+my^2\right)\left(1+\frac{1}{2}y'^2\right)dx\approx$$
$$\approx J_{xI}\int_L\left(1-\frac{1}{2}y'^2+\frac{m}{J_{xI}}y^2\right)dx,$$

consequently

$$J_x\approx J_{xI}\int_L\left(1-\frac{1}{2}y'^2+\frac{y^2}{i_{xI}^2}\right)dx, \qquad (17)$$

where

$$i_{xI}=\sqrt{\frac{J_{xI}}{m}}=\sqrt{\frac{\frac{1}{2}m_2\left(r-h\right)^2+m_1r^2}{m_1+m_2}}$$

is the radius of inertia of the heterogeneous cross section of the rod.

Let, as previously, the elastic line of the rod is described by function (1), then, based on formula (17), the asymptotic expression for the moment of inertia will take the following form:

$$J_x\approx J_{xI}\int_L\left(1-\frac{1}{2}\left(f\frac{\pi}{L}\cos\left(\frac{\pi}{L}x\right)\right)^2+\frac{\left(f\sin\frac{\pi x}{L}\right)^2}{i_{xI}^2}\right)dx,$$

upon integration

$$J_x\approx J_{xI}\left(L-\left(f\frac{\pi}{L}\right)^2\frac{L}{4}+\left(\frac{f}{i_{xI}}\right)^2\frac{L}{2}\right). \qquad (18)$$

A comparative analysis of dependences (16) and (18) shows that the difference between them is observed when the deflection extension exceeds 2,5 m (Fig. 3).

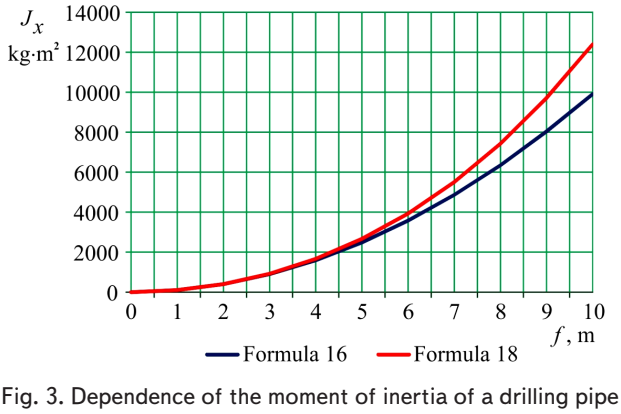

Fig. 3. Dependence of the moment of inertia of a drilling pipe ∅60 on the magnitude of deflection section in a drill string

Typically, the maximum deflection of a drill string in the well is much less than 2,5 m. Based on this, we can conclude that in practical calculations, when $L/f>10$, in order to determine the moments of inertia of the deflected sections of a drill string one can widely apply the simplified (asymptotic) formula (18).

6. Numerical verification of results from the analytical study

As shown above, the moment of inertia of the curved section in a drill string, both in (16) and (18), depends on the parameters that determine both the geometry of its shape and the dimensions of the cross-section. Therefore, for practical calculations, it is also needed to estimate the magnitude of the maximum deflection of the section in a drill string depending on its diameter. To do this, we shall use known ratios between the diameters of drill pipes (DP), weighted drill pipes (WDP), and a bit:

$$\left.\begin{aligned}&d_{\text{WDP}}/D_{\text{b}}=0{,}75\div 0{,}85\ \ \text{at}\ D_{\text{b}}\le 295{,}3\ \text{mm};\\&d_{\text{WDP}}/D_{\text{b}}=0{,}65\div 0{,}75\ \ \text{at}\ D_{\text{b}}>295{,}3\ \text{mm};\\&d_{\text{DP}}/d_{\text{WDP}}=0{,}75\div 0{,}8,\end{aligned}\right\} \qquad (19)$$

where d_{WDP}, d_{DP}, D_{b} are, respectively, the diameter of WDP, DP, and a bit.

The extension of a drill string's section deflection in the well:

$$f=\left(D_{\text{Bh}}-d_{\text{Dl}}\right)/2, \qquad (20)$$

D_{Bh}, d_{Dl} are, respectively, the diameter of the bore hole and a drill lock.

We assume that $D_{\text{Bh}}\approx D_{\text{b}}$; $d_{\text{Dl}}\approx d_{\text{DP}}$. Comparing (19) and (20), after appropriate transformations, we obtain:

– for DP section:

$$\left.\begin{aligned}&f_{\text{DP}}=\left(0{,}236\div 0{,}393\right)d_{\text{DP}}\ \text{at}\ D_{\text{b}}\le 295{,}3\ \text{mm};\\&f_{\text{DP}}=\left(0{,}333\div 0{,}521\right)d_{\text{DP}}\ \text{at}\ D_{\text{b}}>295{,}3\ \text{mm};\end{aligned}\right\} \qquad (21)$$

– for WDP section:

$$\left.\begin{aligned}&f_{\text{WDP}}=\left(0{,}177\div 0{,}314\right)d_{\text{WDP}}\ \text{at}\ D_{\text{b}}\le 295{,}3\ \text{mm};\\&f_{\text{WDP}}=\left(0{,}250\div 0{,}417\right)d_{\text{WDP}}\ \text{at}\ D_{\text{b}}>295{,}3\ \text{mm}.\end{aligned}\right\} \qquad (22)$$

We shall quantitatively and qualitatively verify expression (16) by using data on drill pipes made from different materials. Currently, there is a trend in the development and modernization of drilling equipment towards manufacturing drill pipes from unconventional materials – titanium and fiberglass. Given the scientific and practical interest to their future use, we calculated the moments of inertia for the deflected sections in steel and aluminum, as well as titanium and fiberglass, drill pipes. Accordingly, we accepted the following average values for the density of pipes' material: steel – $\rho_{st}=7850$ kg/m^3, titanium – $\rho_t=4500$ kg/m^3, aluminum – $\rho_{\text{a}}=2700$ kg/m^3, fiberglass – $\rho_{fb}=2000$ kg/m^3. Drilling mud density is $\rho_{\text{p}}=1300$ kg/m^3. Based on (21) and (22), the magnitudes of the maximum deflections of sections are assigned as follows: for DP stage – $f_{\text{DP}}\approx r_{\text{DP}}$, for WDP stage – $f_{\text{WDP}}\approx 0{,}8r_{\text{WDP}}$. Length of deflection halfwaves are as follows: for DP stage – $L_{\text{DP}}=20\div 80$ m, for WDP stage – $L_{\text{WDP}}=10\div 30$ m. The results of numerical calculations of

the moments of inertia for the deflected sections of drill and weighted drill pipes are given in Tables 1, 2. An analysis of formula (16), as well as charts in Fig. 4, 5, show that for a certain length of the halfwave of the section deflection in a string its moment of inertia is in quadratic dependence on the magnitude of the deflection. At the same time, it follows from formula (18) that at the fixed deflection extension the moment of inertia of the deflected section depends linearly on the length of a halfwave (Fig. 6).

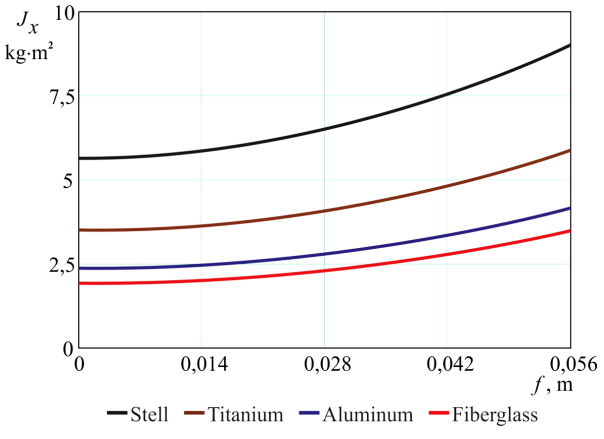

Fig. 4. Dependence of moments of inertia of the deflected sections of DP ((∅114 mm) on a deflection extension

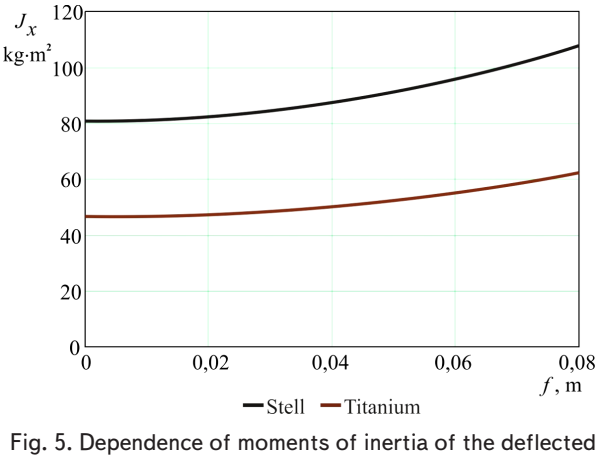

Fig. 5. Dependence of moments of inertia of the deflected sections of WDP ((∅203 mm) on the magnitude of deflection

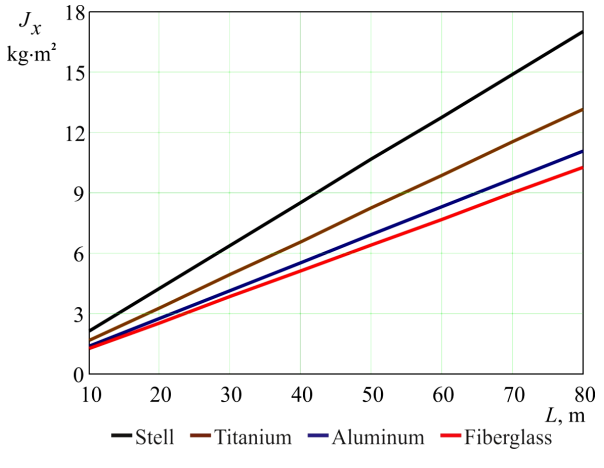

Fig. 6. Dependence of moments of inertia of the deflected sections of DP ((∅114 mm) on the length of a halfwave

Table 1

Moments of inertia for the deflected sections of WDP stage

f	d_{WDP}=108 mm		d_{WDP}=120 mm		d_{WDP}=146 mm	
	Steel	Titanium	Steel	Titanium	Steel	Titanium
L_{WDP}=10 m						
0	2.413	1.386	3.004	1.731	6.946	3.998
0.2r	2.463	1.415	3.067	1.769	7.090	4.083
0.4r	2.611	1.501	3.255	1.880	7.522	4.339
0.6r	2.858	1.646	3.568	2.066	8.242	4.764
0.8r	3.204	1.848	4.007	2.327	9.251	5.360
L_{WDP}=20 m						
f	d_{WDP}=146 mm		d_{WDP}=178 mm		d_{WDP}=203 mm	
	Steel	Titanium	Steel	Titanium	Steel	Titanium
0	13.892	7.996	30.766	17.708	53.884	30.994
0.2r	14.180	8.166	31.404	18.085	54.998	31.650
0.4r	15.044	8.677	33.319	19.216	58.340	33.618
0.6r	16.485	9.529	36.509	21.101	63.909	36.899
0.8r	18.503	10.721	40.976	23.740	71.707	41.492
L_{WDP}=30 m						
f	d_{WDP}=203 mm		d_{WDP}=245 mm		d_{WDP}=273 mm	
	Steel	Titanium	Steel	Titanium	Steel	Titanium
0	80.826	46.491	150.875	87.032	275.717	158.479
0.2r	82.497	47.475	154.035	88.914	281.395	161.813
0.4r	87.510	50.428	163.513	94.562	298.429	171.813
0.6r	95.865	55.349	179.310	103.975	326.819	188.481
0.8r	107.562	62.239	201.426	117.154	366.566	211.815

Based on the numerical data from Tables 1, 2, one should note the following. Increasing the density of a material for drill pipes of the curved section leads to a disproportionate increase in its moment of inertia. This can be explained based on the following considerations. Take for the first case the ratio between the density of steel and fiberglass, which is 3,9 times. At the same time, the ratio between the moments of inertia of the two sections made, respectively, from steel and fiberglass drill pipes is smaller. For example, for DP ∅89 mm (L=40 m) – 2,9÷3,2; for DP ∅114 mm (L=60 m) – 2,6÷3,0; for DP ∅139 mm (L=80 m) – 2,4÷2,7. Consider the second case when the density of steel is 2,25 times greater than the density of titanium. In this case, the ratio between the moments of inertia of two sections made, respectively, from steel and titanium weighted drill pipes is also smaller. For example, for WDP ∅203 mm (L=20 m) – 1,72÷1,74; for WDP ∅273 mm (L=30 m) – 1,73÷1,74.

Based on this analysis, it can be argued that a change in the moment of inertia for the curved sections in a string depends in the first place on the density of pipes' material, with which it is equipped. Changing the moments of inertia of these sections depending on the length of a halfwave of deflection occurs in the same proportion.

Table 2

Moments of inertia for the deflected sections of DP stage

L_{DP}=20 m								
f	d_{DP}=60.3 mm				d_{DP}=73.0 mm			
	Steel	Titanium	Aluminum	Fiberglass	Steel	Titanium	Aluminum	Fiberglass
0	0.251	0.148	0.092	0.070	0.455	0.271	0.172	0.133
0.25r	0.260	0.153	0.096	0.073	0.471	0.281	0.179	0.139
0.5r	0.286	0.169	0.106	0.082	0.519	0.312	0.201	0.157
0.75r	0.329	0.196	0.125	0.097	0.600	0.364	0.237	0.187
r	0.390	0.234	0.150	0.118	0.712	0.436	0.287	0.229
L_{DP}=40 m								
f	d_{DP}=89.0 mm				d_{DP}=101.6 mm			
	Steel	Titanium	Aluminum	Fiberglass	Steel	Titanium	Aluminum	Fiberglass
0	1.694	1.027	0.668	0.528	2.577	1.584	1.050	0.842
0.25r	1.756	1.067	0.697	0.554	2.673	1.648	1.098	0.884
0.5r	1.941	1.190	0.786	0.629	2.960	1.843	1.242	1.009
0.75r	2.249	1.394	0.934	0.755	3.439	2.166	1.482	1.216
r	2.681	1.679	1.141	0.932	4.109	2.619	1.819	1.507
L_{DP}=60 m								
f	d_{DP}=114.3 mm				d_{DP}=127.0 mm			
	Steel	Titanium	Aluminum	Fiberglass	Steel	Titanium	Aluminum	Fiberglass
0	5.630	3.509	2.369	1.925	7.901	4.990	3.427	2.818
0.25r	5.843	3.656	2.480	2.023	8.205	5.204	3.592	2.964
0.5r	6.484	4.097	2.814	2.315	9.120	5.846	4.087	3.402
0.75r	7.550	4.832	3.371	2.803	10.644	6.915	4.912	4.133
r	9.044	5.861	4.151	3.486	12.778	8.412	6.067	5.155
L_{DP}=80 m								
f	d_{DP}=139.7 mm				d_{DP}=168.3 mm			
	Steel	Titanium	Aluminum	Fiberglass	Steel	Titanium	Aluminum	Fiberglass
0	14.342	9.178	6.402	5.323	26.372	17.341	12.489	10.602
0.25r	14.905	9.579	6.717	5.604	27.441	18.129	13.125	11.179
0.5r	16.593	10.783	7.661	6.446	30.650	20.491	15.032	12.909
0.75r	19.406	12.789	9.233	7.851	35.998	24.428	18.211	15.793
r	23.345	15.598	11.435	9.816	43.486	29.940	22.661	19.831

7. Discussion of results of studying the moment of inertia for the curved section in a drill string at its rotation

The proposed analytical approaches to the evaluation of moments of inertia for the curved sections in a drill string at its rotation can be implemented in two ways. The advantages of these techniques are a relatively simple mathematical apparatus, as well as the fact that the results from one technique can always be confirmed by the results from another technique. The results obtained from calculating the moments of inertia for the curved sections, equipped with steel, aluminum, titanium or fiberglass pipes, can be applied in the further research. Important in this regard is an analysis of the stressed-strained state of a drill string's elements, refinement of energy costs on the process of rotation of curved sections in a well, as well as analysis of the critical frequencies of rotation.

Under actual conditions, the eccentric rotation of curved sections in a string at frequencies close to critical is characterized by a transition to an unsteady state, predetermined by the occurrence of transverse oscillations and "running" waves. Approaching the critical frequencies always leads to an increase in the number of halfwaves in deformation, and, accordingly, in the number of deflected sections in a drill string. The new steady position with the increased number of halfwaves of deformation forms at the frequency of rotation, which is greater than the critical. Therefore, to determine the difference between the "operating" and critical frequencies of rotation of the deformed drill string, we plan further studies in the future.

The disadvantage of our study is the lack of practical test of the established analytical dependences experimentally. This is explained by the absence of specialized measuring borehole equipment and the impossibility of its application under industrial conditions. However, the research results obtained when using a model with the distributed mass are in good agreement with the results of studies, reported in [31, 32], by applying a finite element method.

The advantage of the dependences established in the course of our study is the high accuracy of results and the ease of their application in practical calculations at drilling enterprises. Employing them could help assess more accurately the dynamic stability and pliability of a drill string under conditions of a vibration load at rotor and rotor-turbine drilling techniques. Studies into such an aspect could address the elucidation of the magnitude of consumption of mechanical energy on pushing and turning the curved sections in a drill string, as well as searching for energy-saving modes of its operation. In this regard, there are remaining complex and relevant issues related to analytical and nu-

merical modeling of oscillatory processes of a drill string when drilling conditional-vertical, inclined-directed, and horizontal wells.

8. Conclusions

An analysis of the derived research results testifies to that an increase in the density of a material for the curved section of WDP by 2,25 times leads to an increase in its moments of inertia by 1,7 times, while at the same time increasing the density of a material for the curved section of DP by 3.9 times on average increases its moment of inertia by 2,4÷3,2 times.

The study that we performed has also shown that the analytical evaluation of inertial properties of the curved sections belongs to a different scale of motion or a scale of the deformed state of a drill string. It turned out that the results obtained from simple models are applicable only in cases when a curvilinear section of a drill string undergoes large displacements (lift extension is larger or significantly larger than the transverse size of the string). Only in this case one can obtain values for the moments of inertia with a sufficient degree of accuracy. For the case of small displacements (when a lift extension of the curvilinear section is less than, or comparable to, a transverse size of the string), it is necessary to apply those dependences that were derived when using a model with distributed parameters.

References

1. Unveiling complexity of drill–string vibrations: Experiments and modeling / Kapitaniak M., Vaziri Hamaneh V., Páez Chávez J., Nandakumar K., Wiercigroch M. // International Journal of Mechanical Sciences. 2015. Vol. 101-102. P. 324–337. doi: https://doi.org/10.1016/j.ijmecsci.2015.07.008
2. Zhu X., Tang L., Yang Q. A Literature Review of Approaches for Stick-Slip Vibration Suppression in Oilwell Drillstring // Advances in Mechanical Engineering. 2014. Vol. 6. P. 967952. doi: https://doi.org/10.1155/2014/967952
3. Gulyayev V. I., Hudoliy S. N., Glushakova O. V. Simulation of torsion relaxation auto-oscillations of drill string bit with viscous and Coulombic friction moment models // Proceedings of the Institution of Mechanical Engineers, Part K: Journal of Multi-body Dynamics. 2011. Vol. 225, Issue 2. P. 139–152. doi: https://doi.org/10.1177/1464419311405571
4. Ghasemloonia A., Geoff Rideout D., Butt S. D. A review of drillstring vibration modeling and suppression methods // Journal of Petroleum Science and Engineering. 2015. Vol. 131. P. 150–164. doi: https://doi.org/10.1016/j.petrol.2015.04.030
5. Velichkovich A., Dalyak T., Petryk I. Slotted shell resilient elements for drilling shock absorbers // Oil & Gas Science and Technology – Revue d'IFP Energies nouvelles. 2018. Vol. 73, Issue 34. doi: https://doi.org/10.2516/ogst/2018043
6. Pryhorovska T. Rock heterogeneity numerical simulation as a factor of drill bit instability // Engineering Solid Mechanics. 2018. P. 315–330. doi: https://doi.org/10.5267/j.esm.2018.8.002
7. Goloskov E. G., Filippov A. P. Nestacionarnye kolebaniya deformiruemyh sistem. Kyiv: Naukova dumka, 1977. 339 p.
8. Pukach P. Y. On the unboundedness of a solution of the mixed problem for a nonlinear evolution equation at a finite time // Nonlinear Oscillations. 2012. Vol. 14, Issue 3. P. 369–378. doi: https://doi.org/10.1007/s11072-012-0164-6
9. Velichkovich A. S., Popadyuk I. I., Shopa V. M. Experimental study of shell flexible component for drilling vibration damping devices // Chemical and Petroleum Engineering. 2011. Vol. 46, Issue 9-10. P. 518–524. doi: https://doi.org/10.1007/s10556-011-9370-9
10. Sesyunin N. A. Ob izgibe vesomogo sterzhnya v naklonnoy cilindricheskoy polosti // Izv. vuzov. Neft' i gaz. 1983. Issue 9. P. 22–25.
11. Royzman V. P. Possibility of creating non-resonance design, non-critical rotors and rods stable to compression // Vibracii v tekhnike i tekhnologiyah. 2015. Issue 3 (79). P. 38–43.
12. Velichkovich A. S., Dalyak T. M. Assessment of Stressed State and Performance Characteristics of Jacketed Spring with a Cut for Drill Shock Absorber // Chemical and Petroleum Engineering. 2015. Vol. 51, Issue 3-4. P. 188–193. doi: https://doi.org/10.1007/s10556-015-0022-3
13. Some aspects of design and application of inertial dampers / Dutkiewicz M., Gołębiowska I., Shatskyi I., Shopa V., Velychkovych A. // MATEC Web of Conferences. 2018. Vol. 178. P. 06010. doi: https://doi.org/10.1051/matecconf/201817806010
14. Velichkovich A. S. Shock Absorber for Oil-Well Sucker-Rod Pumping Unit // Chemical and Petroleum Engineering. 2005. Vol. 41, Issue 9-10. P. 544–546. doi: https://doi.org/10.1007/s10556-006-0015-3
15. Gołębiowska I., Dutkiewicz M. The effectiveness of vibration damper attached to the cable due to wind action // EPJ Web of Conferences. 2017. Vol. 143. P. 02029. doi: https://doi.org/10.1051/epjconf/201714302029
16. Frictional Interaction of a Cylindrical Shell with Deformable Filler Under Nonmonotonic Loading / Popadyuk I. Y., Shats'kyi I. P., Shopa V. M., Velychkovych A. S. // Journal of Mathematical Sciences. 2016. Vol. 215, Issue 2. P. 243–253. doi: https://doi.org/10.1007/s10958-016-2834-x
17. Panevnik D. A., Velichkovich A. S. Assessment of the stressed state of the casing of the above-bit hydroelevator // Oil Industry Journal. 2017. Vol. 1. P. 70–73.
18. Kukhar V., Balalayeva E., Nesterov O. Calculation method and simulation of work of the ring elastic compensator for sheet-forming // MATEC Web of Conferences. 2017. Vol. 129. P. 01041. doi: https://doi.org/10.1051/matecconf/201712901041
19. Shatskyi I., Popadyuk I., Velychkovych A. Hysteretic Properties of Shell Dampers // Springer Proceedings in Mathematics & Statistics. 2018. P. 343–350. doi: https://doi.org/10.1007/978-3-319-96601-4_31
20. Shatskii I. P., Perepichka V. V. Shock-wave propagation in an elastic rod with a viscoplastic external resistance // Journal of Applied Mechanics and Technical Physics. 2013. Vol. 54, Issue 6. P. 1016–1020. doi: https://doi.org/10.1134/s0021894413060163

21. Shatskyi I., Perepichka V. Problem of Dynamics of an Elastic Rod with Decreasing Function of Elastic-Plastic External Resistance // Springer Proceedings in Mathematics & Statistics. 2018. P. 335–342. doi: https://doi.org/10.1007/978-3-319-96601-4_30
22. Levchuk K. G. Engineering Tools and Technologies of Freeing of the Stuck Metal Drilling String // METALLOFIZIKA I NOVEISHIE TEKHNOLOGII. 2018. Vol. 40, Issue 1. P. 45–137. doi: https://doi.org/10.15407/mfint.40.01.0045
23. Kryzhanivs'kyi E. I., Rudko V. P., Shats'kyi I. P. Estimation of admissible loads upon a pipeline in the zone of sliding ground // Materials Science. 2004. Vol. 40, Issue 4. P. 547–551. doi: https://doi.org/10.1007/s11003-005-0076-z
24. Shats'kyi I. P., Struk A. B. Stressed state of pipeline in zones of soil local fracture // Strength of Materials. 2009. Vol. 41, Issue 5. P. 548–553. doi: https://doi.org/10.1007/s11223-009-9165-9
25. Vazouras P., Karamanos S. A., Dakoulas P. Mechanical behavior of buried steel pipes crossing active strike-slip faults // Soil Dynamics and Earthquake Engineering. 2012. Vol. 41. P. 164–180. doi: https://doi.org/10.1016/j.soildyn.2012.05.012
26. Zhang J., Liang Z., Han C. J. Finite element analysis of wrinkling of buried pressure pipeline under strike-slip fault // Mechanics. 2015. Vol. 21, Issue 3. doi: https://doi.org/10.5755/j01.mech.21.3.8891
27. Shats'kyi I. P., Lyskanych O. M., Kornuta V. A. Combined Deformation Conditions for Fatigue Damage Indicator and Well-Drilling Tool Joint // Strength of Materials. 2016. Vol. 48, Issue 3. P. 469–472. doi: https://doi.org/10.1007/s11223-016-9786-8
28. Improving the aluminum drill pipes stability by optimizing the shape of protector thickening / Vlasiy O., Mazurenko V., Ropyak L., Rogal A. // Eastern-European Journal of Enterprise Technologies. 2017. Vol. 1, Issue 7 (85). P. 25–31. doi: https://doi.org/10.15587/1729-4061.2017.65718
29. Vytvytskyi I. I., Seniushkovych M. V., Shatskyi I. P. Calculation of distance between elastic-rigid centralizers of casing // Naukovyi Visnyk Natsionalnoho Hirnychoho Universytetu. 2017. Issue 5. P. 29–35.
30. Orynyak I. V., Radchenko S. A., Batura A. S. Calculation of free and forced vibrations of a pipeline system. Part 1. The analysis of vibrations of a spatial rod system // Problemy prochnosti. 2007. Issue 1. P. 79–93.
31. Introduction to Rotor Dynamics. URL: http://www.springer.com/cda/content/document/cda_downloaddocument/9781447142393-c2.pdf?SGWID=0-0-45-1334803-p174512894
32. Tadeo A. T., Cavalca K. L. A Comparison of Flexible Coupling Models for Updating in Rotating Machinery Response // Journal of the Brazilian Society of Mechanical Sciences and Engineering. 2003. Vol. XXV, Issue 3. P. 235–246. URL: http://www.scielo.br/pdf/jbsmse/v25n3/a04v25n3.pdf
33. Developing a method for the assessment of axial load in arbitrary cross-sections of the column of pumping rods / Andrusyak A., Grydzhuk J., Dzhus A., Steliga I. // Eastern-European Journal of Enterprise Technologies. 2017. Vol. 1, Issue 7 (85). P. 32–37. doi: https://doi.org/10.15587/1729-4061.2017.92860
34. Saroyan A. E. Teoriya i praktika raboty buril'noy kolonny. Moscow: Nedra, 1990. 263 p.